

10

Large-scale Controls on Cloudiness

Christopher S. Bretherton and Dennis L. Hartmann

Department of Atmospheric Sciences, University
of Washington, Seattle, WA, U.S.A.

Abstract

The climatological distribution of clouds is tightly coupled to large-scale circulation. Net cloud radiative forcing is mainly the result of boundary layer clouds in large-scale subsidence. Deep convective cloud systems exert long- and shortwave cloud forcing that nearly cancel out each other. The extent of this cancellation depends strongly on the vertical motion profile, suggesting that if the cancellation is not coincidental, dynamic feedbacks probably play a role in its maintenance. Low cloud radiative forcing is tied to how cold the surface is compared to the free troposphere. It is an open question how this correlation should be represented in a way that generalizes to a perturbed climate. Simple empirical representations of deep and low cloud forcing are shown to provide strong feedbacks on an idealized model of a tropical overturning circulation. Global weather and climate models, however, still have profound difficulties in accurately representing the cloud response to large-scale forcings.

Introduction

Clouds result from the condensation of water vapor. Since cloud particles generally sediment and tend to evaporate in subsiding air, clouds are most frequently observed in regions where the motion has been upward; this can both act to induce supersaturation as a result of adiabatic cooling and to lift condensed water higher in the atmosphere. However, regions of time-mean subsidence are not necessarily cloud-free, because vertical motion is organized on many scales: from turbulent eddies to moist convection to transient storm systems. In addition, the microphysical diversity and complexity of clouds makes their response to a given pattern of vertical motion challenging to model. Thus atmospheric general circulation models (GCMs) struggle to simulate skillfully the relationships between cloudiness and its large-scale controls in the current

climate and how this will change in climates perturbed by changed greenhouse gas or aerosol concentrations.

In this chapter, we relate some observed aspects of cloud climatology to their dynamic controls. We describe the impact of empirically deduced radiative feedbacks from deep convective clouds and from boundary layer clouds in an idealized model of the tropical Walker circulation. On this basis, we examine the physical nature of the deep and low cloud radiative forcing (CRF) parameterizations, and whether they might generalize to other climates. We conclude with a discussion of the modeling challenges and biases in simulating the relation between cloudiness and large-scale circulations.

Large-scale Climatology of Cloudiness

The planetary-scale organization of cloudiness can easily be seen by comparing global maps of cloud properties with global maps of time-mean vertical motion. Figure 10.1 shows the annual mean distribution of total cloud amount from the International Satellite Cloud Climatology Project (ISCCP) (Rossow and Schiffer 1999). The biggest cloudiness maxima are over the extratropical oceans, where baroclinic eddies drive substantial vertical motion over the moist surface of the ocean. Also evident is a banded structure in which the upward motion near the equator enhances cloud fraction; the downward motion in the subtropics generally suppresses cloudiness, except at the eastern margins of the subtropical oceans where it combines with low sea surface temperature (SST) to form the ideal environment for marine stratocumulus clouds, which are trapped under an inversion that is supported by large-scale downward

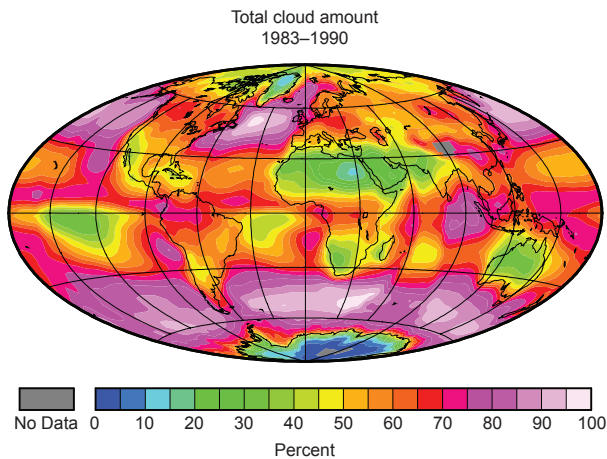


Figure 10.1 Annual mean total cloud fraction from ISCCP.

motion. The contribution of satellite-visible low-topped marine boundary layer clouds to the total cloudiness (Figure 10.2) maximizes in these regions and over the extratropical oceans, especially during summertime (Klein and Hartmann 1993). Extensive stratus clouds and fog form in regions of warm advection, while stratocumulus and shallow cumulus clouds are ubiquitous in the downward mean motion and cold advection behind cold fronts associated with midlatitude storms.

A cursory examination of the spatial organization of clouds shows a strong relationship to the general circulation of the atmosphere. Less immediately apparent is the strong role of radiative processes in controlling these distributions. Deep convection drives strong latent heating and large-scale upward motion. By mass continuity, an equal amount of downward mass flux must exist somewhere away from the convection. Energy conservation requires that globally averaged heating of the atmosphere through latent heat release must be balanced by radiative cooling of the atmosphere (aside from a small residual resulting from upward surface sensible heat flux).

These arguments show that latent heating rate and thereby global-scale precipitation and evaporation are constrained by the radiative cooling rate of the atmosphere rather than by surface humidity. These two quantities respond quite differently to climate perturbations, even though most of the radiative cooling comes from emission from water vapor and clouds. This can lead to important large-scale constraints on convective cloud structures (Hartmann and Larson 2002), as well as on the sensitivity of precipitation and evaporation rates to global mean surface temperature (Held and Soden 2006). Hartmann and Larson (2002) argued that the balance between clear-sky radiative cooling and convective heating suggests that the tops of anvil clouds in the tropics should

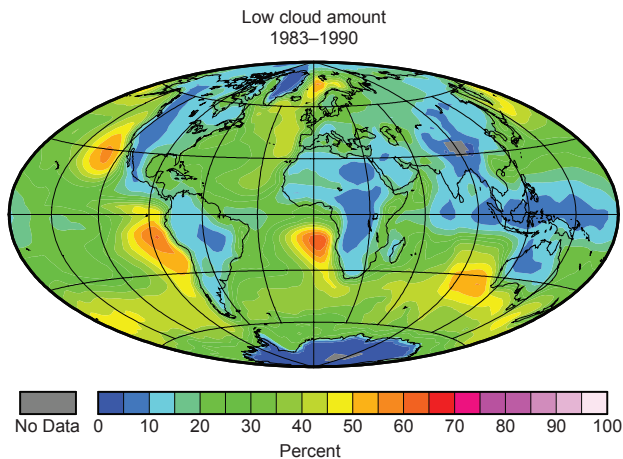


Figure 10.2 Annual mean fractional coverage of low-topped clouds with cloud-top pressures greater than 680 hPa from ISCCP.

remain at a constant temperature under climate change. In addition, radiative cooling (and hence the atmospheric circulation and clouds) can be affected immediately by greenhouse gas perturbations, even before they have induced a change in surface temperature and humidity (Gregory and Webb 2008).

Net Radiative Effect of Cloudiness

One way to measure the importance of clouds is to assess their impact on the radiation balance at the top of the atmosphere. Clouds affect both solar and terrestrial radiation transmission. The effect on the top-of-atmosphere (TOA) radiation balance depends on the radiative properties of the cloud particles and the morphology of the cloud. To a first order, the reduction of net upward long-wave radiative flux attributable to clouds, or longwave cloud radiative forcing (LWCRF), depends on the cloud-top temperature at TOA. It is usually positive and largest for clouds with high, cold tops. The shortwave cloud radiative forcing (SWCRF) is usually negative at TOA because clouds reflect sunlight. SWCRF depends on the liquid and ice water path and, secondarily, on cloud particle size and habit. The sum of LWCRF and SWCRF at TOA is the net CRF (NCRF). The left panel of Figure 10.3 shows that the NCRF of an idealized tropical cloud layer increases as its cloud-top temperature cools and decreases as its optical depth increases. High clouds in the tropics can have either strong warming or cooling effects on the TOA radiation budget, depending on the optical depth of the clouds. Low-topped clouds always have a net radiative cooling effect.

The right panel of Figure 10.3 shows the fractional coverage of clouds in the East Pacific with visible optical depths in logarithmic categories and in 5°C intervals of cloud-top temperature as measured by MODIS. The volume under this histogram is approximately equal to the total cloud fraction. Large amounts of cloud are present with both positive and negative NCRF, and the net effect of tropical convective cloud systems is fairly small. Later, we will return to this observation (namely, that short- and longwave CRF of tropical oceanic deep convection cancel surprisingly well) and look at its dynamic implications to ask whether this is a mere coincidence of the current climate.

In this region, boundary layer clouds with tops at high temperatures are also common, and the probability distribution function (PDF) of their optical depth integrates to have a strong negative NCRF. The net negative global effect of clouds on the Earth's energy balance can be attributed primarily to marine boundary layer clouds.

Large-scale Vertical Velocity Profiles and Cloud Properties

In the tropics, a tight relationship exists between the vertical structure of deep convective cloud ensembles, their radiative effects, and the vertical structure

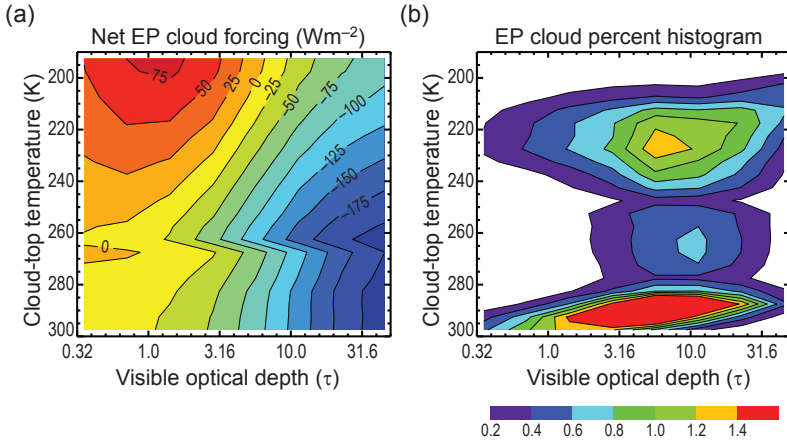


Figure 10.3 (a) Net effect of tropical clouds on the top-of-atmosphere radiation budget as a function of cloud-top temperature and cloud optical depth. (b) MODIS-derived histogram of East Pacific (EP) ITCZ cloud cover (in units of percent cloud fraction per bin) binned jointly by visible optical depths (in logarithmic categories) and cloud-top temperature (in $5^{\circ}C$ intervals) (Kubar et al. 2007).

of the vertical velocity field. Climatological profiles of vertical pressure velocity, ω , show “top heavy” upward motion in the West Pacific warm pool and “bottom heavy” upward motion in the East Pacific ITCZ (Back and Bretherton 2006; Yuan and Hartmann, submitted), as shown in Figure 10.4a, b. Back and Bretherton (submitted) have correlated this to the lower SST and stronger meridional SST gradients in the East Pacific. Figure 10.4 also shows that different reanalyses have a large spread in the amplitude of the 850 hPa upward motion in the East Pacific ITCZ, even though all have similar vertical motion profiles. This illustrates that there are not enough observations to prevent large uncertainties in reanalysis-derived vertical motion in the tropics. Presumably, this reflects differences in the moist physical parameterizations (especially for deep convection) between the forecast models that are used for creating the reanalyses. On daily timescales, this problem becomes even more severe and needs to be kept in mind when correlating observed cloud properties with vertical motion.

In the tropical free troposphere, the adiabatic cooling attributable to vertical motion closely counterbalances diabatic heating, which in rainy regions derives primarily from latent heating and secondarily from radiation. Bottom-heavy upward motion implies bottom-heavy latent heating, which requires more shallow cumuli and less deep convection. Indeed, on average, cloud ensembles in the East Pacific ITCZ have less LWCRF per (negative) unit of SWCRF, and a stronger negative effect on the radiation balance, than cloud ensembles in the West Pacific ITCZ (Kubar et al. 2007), as shown in Figure 10.4c. This demonstrates how important it is, when interpreting cloud observations, to consider

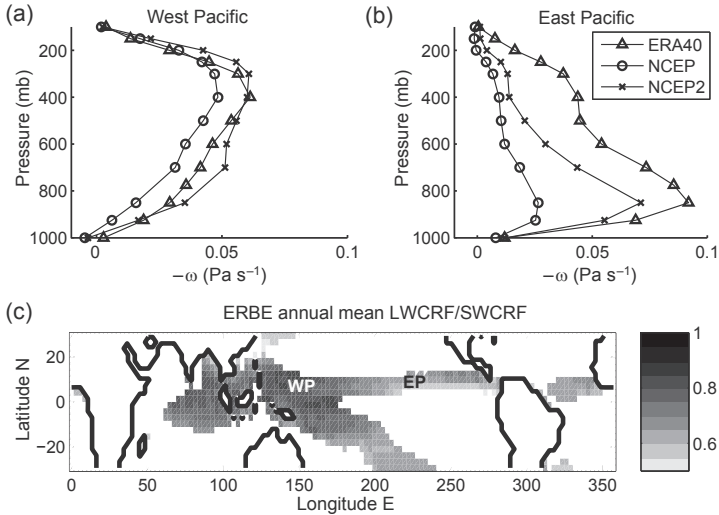


Figure 10.4 Annual mean vertical motion profiles in (a) West Pacific (WP) and (b) East Pacific (EP) based on three reanalyses. ERBE-deduced annual mean LWCRF/SWCRF ratio is shown in (c); WP and EP are marked. Panels (a) and (b) were adapted from Fig. 3 in Back and Bretherton (2005).

carefully the dynamic regime from which they are taken. When analyzed in this way, observations provide a tighter constraint on GCM simulations of clouds and their radiative forcing.

Observations show clearly that the large-scale velocity field, the general circulation, and the associated convection and cloud properties are closely linked. Large-scale dynamic processes and the constraints that the radiation budget imposes on clouds and circulation are important. Changes in the large-scale circulation that accompany climate change are likely to feed back strongly on cloud properties. Expected climate responses to global warming, such as a weakened Walker circulation in the tropics (Vecchi et al. 2006), an expanded Hadley cell (Seager et al. 2007), and northward shifting of storm tracks (Yin 2005), are likely to produce significant cloud feedbacks. In addition, clouds will both respond and feed back on the distribution of SST within the tropics as it changes under global warming or in response to aerosols, with a significant influence on global CRF. The response of convective and marine boundary layer clouds is likely to be affected by changes in SST gradients in the tropics, and this may have a significant effect on the TOA radiation budget (Barsugli et al. 2006; Zhu et al. 2007).

Cloud-radiative Feedbacks on Tropical Circulations

In the preceding section, we documented how vertical motion controls clouds on large space and timescales. Here, we discuss radiative feedbacks of clouds

on the large-scale circulation and the associated surface temperature gradients. Our focus is on the tropical oceans, where SST and rainfall biases in coupled GCMs (e.g., insufficiently cool SSTs under the eastern subtropical oceans, spurious eastern Pacific double ITCZ) have often been attributed to cloud feedbacks.

Peters and Bretherton (2005) showed the effect of cloud feedbacks on an idealized model of the tropical Walker circulation above a slab ocean. The tropical troposphere was represented with a single mode of vertical motion following Neelin and Zeng (2000) and included simplified feedbacks between conditional instability, convection, clouds, water vapor, and surface/TOA radiation. They modeled an east–west slice along the equatorial Pacific. The circulation was forced by removing heat from the eastern part of the slab ocean (representing equatorial upwelling) but not from the west. Clearly this type of model cannot represent the differences between bottom-heavy and top-heavy vertical motion profiles and shallower versus deeper precipitating cumuli that are seen over the tropical oceans (e.g., Takayabu and Masunaga, this volume). However, because it is simple, it can illuminate some of the fundamental mechanisms by which clouds radiatively influence tropical general circulation.

Peters–Bretherton Representation of Cloud Radiative Effects

Two cloud-radiative feedbacks are considered in the Peters–Bretherton (2005) model. For consistency, we will follow their sign conventions, even though other conventions might be more natural for the discussion here. The atmospheric CRF, $-R^{cld}$, is defined as the radiative heating of the atmospheric column attributable to the presence of cloud. The surface CRF, S^{cld} , is defined as the radiative heating of the surface as a result of the presence of cloud. They used empirical fits to satellite observations to relate these radiative forcings to large-scale predictors. These fits are of independent interest, as they encapsulate the primary radiative effects of low-latitude oceanic clouds on the real tropical atmosphere–ocean system.

Peters and Bretherton distinguished between deep convective clouds in rainy regions and boundary layer clouds in dry regions, which have rather different radiative effects. They found that on monthly timescales and synoptic space scales, deep convective cloud radiative effects scale with precipitation, whereas boundary layer CRFs scale with lower tropospheric stability (LTS).

Figure 10.5a, b shows the satellite-derived atmospheric radiative heating, $-R^{cld}$, and surface cloud radiative cooling, $-S^{cld}$ (from ISCCP-FD; Zhang et al. 2004) versus monthly precipitation, P (from Xie and Arkin 1997). All of these fields have retrieval uncertainties discussed in the references above, but are thought to be accurate to 10–20% at most locations. Each point is a climatological monthly average over a $2.5^\circ \times 2.5^\circ$ grid box over the tropical oceans (20°S – 20°N); L is the latent heat of vaporization. To the right of the vertical

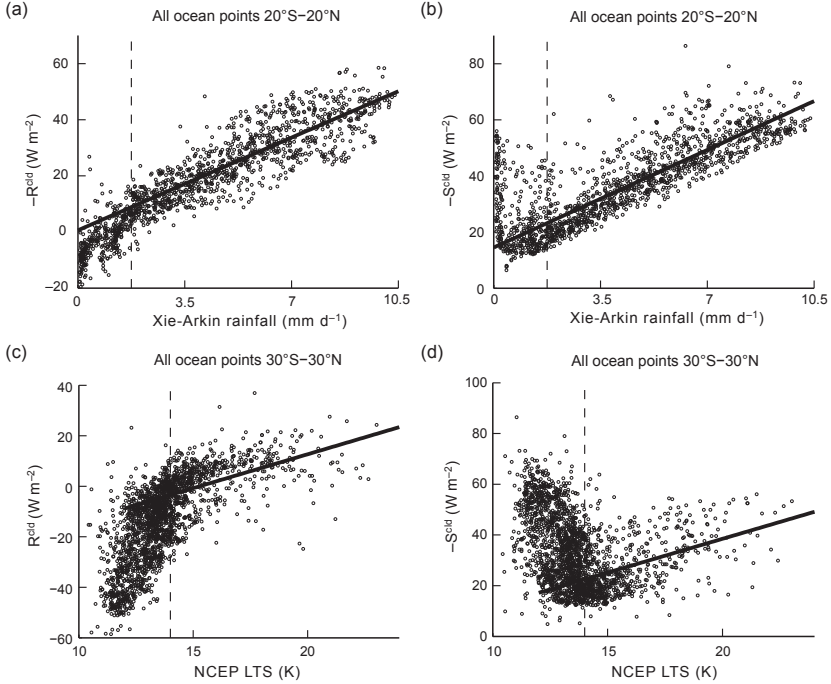


Figure 10.5 Scatterplots (a) and (b) represent low-latitude ocean gridpoints of monthly mean satellite-derived cloud-induced atmospheric column radiative heating, $-R^{cld}$, and surface radiative cooling, $-S^{cld}$, versus rainfall. Fit lines are superposed. The same is shown in (c) and (d) but for lower tropospheric stability (LTS), with fit lines superposed. In (c), R^{cld} is plotted instead of $-R^{cld}$ because boundary layer clouds tend to produce atmospheric radiative cooling at high LTS. In each plot, the fit is best to the right of the dashed line, which marks an approximate climatological threshold between deep convection and boundary layer clouds. Adapted from Peters and Bretherton (2005).

dashed line, in regions of significant deep convective rainfall, the data are well fit by the linear relationships:

$$-R^{cld} = rLP, \quad (10.1a)$$

$$-S^{cld} = 17 \text{ W m}^{-2} + rLP, \quad (10.1b)$$

where $r=0.17$ and $P>1.8 \text{ mm d}^{-1}$. These can be interpreted as anvil cirrus-induced greenhouse heating of the atmosphere and shading of the sea surface from deep convection, both increasing at the same rate with rainfall. Together, Equations 10.1a and 10.1b imply that the net TOA CRF in rainy regions of the tropical oceans is $S^{cld} - R^{cld} \approx -17 \text{ W m}^{-2}$, independent of the amount of deep convection as measured by rainfall rate, a result which we will return to below. Equation 10.1a also implies that the cloud-induced atmospheric radiative heating in deep convective regions is a constant and non-negligible fraction r of the latent heating LP of the atmospheric column. These fits are tropics-wide

composites. Local deviations from these fits are caused by the vertical structure (top heaviness) of the cloud cover, effects of wind shear on upper-level clouds, and other factors.

Lower tropospheric stability, $LTS = \theta(700 \text{ hPa}) - \theta(1000 \text{ hPa})$, is a good predictor of boundary layer cloud amount. Klein and Hartmann (1993) documented that stratus cloud amount is correlated to LTS, both seasonally and geographically. LTS is also a good predictor of both atmospheric and surface cloud radiative cooling over the low-latitude oceans, as seen in Figure 10.5c, d. In Figure 10.5c, the vertical axis is R^{cd} , whereas in Figure 10.5a it was $-R^{cd}$. Peters and Bretherton (2005) made this choice because in contrast to deep convective clouds, boundary layer clouds cool the atmosphere ($R^{cd} > 0$).

Figure 10.5c, d shows two regimes separated by a threshold lower tropospheric stability, $LTS_d = 14 \text{ K}$ (dashed line). The regime $LTS < LTS_d$ left of the dashed line corresponds to deep convection, which we have already considered. Over the warmest oceans, LTS is the lowest and rainfall is the highest; thus Figure 10.5c, d shows another view of the same behavior depicted in Figure 10.5a, b. Where $LTS > LTS_d$, right of the dashed line, deep convection is rare and boundary layer clouds dominate. Here, the following empirical linear fits apply:

$$R^{cd} = 3 + \sigma(LTS - LTS_d), \quad (10.2a)$$

$$-S^{cd} = 22 + \sigma(LTS - LTS_d), \quad (10.2b)$$

where $\sigma = 3 \text{ W m}^{-2} \text{ K}^{-1}$. The ocean experiences net cloud-induced cooling ($-S^{cd} > 0$) because of cloud shading, partly compensated by a cloud-induced increase in downwelling longwave radiation. The atmosphere experiences net cooling ($R^{cd} > 0$) as a result of cloud enhancement of longwave radiative cooling. Both the ocean and atmospheric cloud radiative cooling increase at about the same rate with LTS.

Response of the Peters–Bretherton Model to Cloud Radiative Feedbacks

The Peters–Bretherton model exhibits important model sensitivity to both deep convective and boundary layer cloud radiative feedbacks. Figure 10.6 compares steady-state solutions with no cloud radiative feedbacks, radiative feedbacks attributable only to the deep convective clouds, and radiative feedbacks as a result of both deep convective and low boundary layer clouds. The left edge of the domain is the warm pool; the right edge is the cold pool, where energy is being withdrawn more quickly from the ocean mixed layer. Over the warm pool, the model forms a region of ascent, deep convection, and rainfall separated by a sharp edge from a region of mean subsidence and no precipitation over the cold pool. The deep convective cloud feedback has no impact on the pattern of mean vertical motion (left panel) or rainfall, but flattens the SST gradients over the warm, rainy regions (center panel). The boundary layer cloud

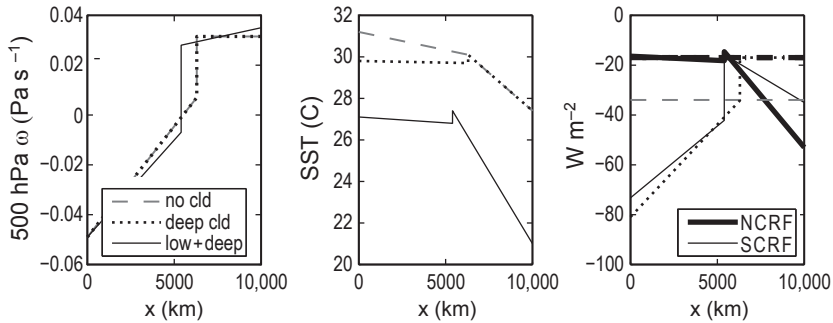


Figure 10.6 Steady state 500 hPa ω (left), sea surface temperature (SST) (center), and net and surface cloud radiative forcing (CRF) (right) in the Peters–Bretherton model, forced by heat removal from the ocean mixed layer that linearly increases from 0 at the left edge to 80 W m^{-2} at the right edge. Dashed line: no cloud feedbacks (horizontally uniform CRF); chain-dash: only deep cloud feedbacks; solid line: low and deep cloud feedbacks. Rainfall (mm d^{-1}) is approximately $160(0.03 - \omega_{500})$.

feedback significantly cools SST over the East Pacific, further enhancing the low cloud cover there, intensifying the Walker circulation, and narrowing and slightly cooling the rainy region.

In both cases, the clouds feed back on the atmospheric circulation by their net TOA radiative effect (NCRF, right panel). The circulation diverts energy out of regions of atmospheric ascent into regions of descent. Extra local TOA radiative cooling must be compensated by more advective energy import, which requires stronger subsidence. Hence, the TOA radiative energy loss that results from boundary layer clouds over the cool SST regions strengthens the subsidence there. Deep convective clouds have no TOA radiative effect, hence no effect on the circulation in this model.

The SST adjusts to balance the surface energy budget. More deep convection reduces surface insolation (a negative surface cloud radiative forcing, or SCRF, visible in the right panel). This cirrus anvil shading effect is a powerful negative feedback on further SST rise. Ramanathan and Collins (1991) suggested that this feedback would keep the warmest tropical SSTs fixed close to 30°C even in highly perturbed climates, keeping tropical climate sensitivity very weak. Waliser and Graham (1993) and others pointed out the correct interpretation; namely, that the shading feedback keeps the warmest SSTs (now 30°C) from substantially exceeding the threshold SST for deep convection (now 26°C). Given a forcing such as CO_2 doubling, the threshold SST adjusts as much as is needed to bring the global energy budget into balance.

In summary, in a simple model, horizontal gradients in TOA cloud radiative forcing act as atmospheric circulation feedbacks, and cloud shading helps regulate SST. We believe that these ideas can also serve as useful guides for thinking about the real atmosphere.

Generality of Cloud Relationships versus the Large Scale

The two empirical relationships shown in Equations 10.1 and 10.2 between clouds and their large-scale environment are interesting features of the current climate. Can they also be generalized to perturbed (e.g., ice age or greenhouse) climates? If so, this would provide powerful constraints on low-latitude climate sensitivity. Because we cannot observe other climates, this question must be addressed either through physical arguments that transcend the current climate or through detailed and trustworthy process models that reproduce these relationships. In neither case is the answer yet conclusive, but the physical arguments are worth reviewing.

Balance of LWCRF and SWCRF in Tropical Oceanic Deep Convection

If LWCRF and SWCRF stayed roughly balanced over marine deep convection regions in a changed climate, then any tropical-mean NCRF change could not come from these regions. There is not enough deep convective area or boundary layer cloud over tropical land masses to affect tropics-wide NCRF to a large extent. Thus tropical NCRF changes would have to come mainly from boundary layer cloud regimes.

This idea is consistent with intercomparisons of IPCC AR4-coupled global climate models. Bony and DuFresne (2005) analyzed simulations with 15 atmospheric models using specified historical SSTs, aggregating the model cloud response using tropical (30°S–30°N) vertical velocity binning. They found that the interannual variability in binned NCRF was caused primarily by subsidence regions, and that different GCMs produced substantially different levels of interannual variability in those regions. They also analyzed the NCRF change associated with equilibrium CO₂ doubling in coupled versions of these models. Again, the change was larger and showed larger intermodel differences in subsidence regions. They concluded that boundary layer clouds, especially trade cumulus regimes which cover much of the subtropical oceans, are the principal cause of tropical NCRF changes. However, cloud formation from deep convection in GCMs relies on a cascade of uncertain parameterizations, so model consensus is an unsatisfying and perhaps unreliable substitute for a physical argument.

Even in the current climate, the balance of LWCRF and SWCRF holds only when we aggregate in time and space. As pointed out earlier, the ratio of LWCRF to SWCRF is affected by dynamics, because the vertical distribution of clouds is tightly linked to the mean vertical motion profile. Thus, it is only appropriate to talk of a balance after averaging across the vertical velocity regimes seen over the tropical rainfall belts. Over land, deep-convective SWCRF tends to exceed LWCRF, perhaps because of the diurnal cycle or perhaps for microphysical reasons.

Kiehl (1994) suggested that the balance is a coincidence of the current climate that stems from the typical optical thickness and cloud-top temperature of cirrus anvils. If so, there is no reason to think the changes of LWCRF and SWCRF would track each other in a future climate. Hartmann et al. (2001) suggested that it may be maintained dynamically by the relative inefficiency of horizontal energy exchange between atmospheric columns in deep convective regions, and hence would hold in other climates. Further study of these two hypotheses seems warranted, given their different implications for the role of deep convection in climate sensitivity.

This is most feasible within the model world. The Hartmann et al. (2001) hypothesis should apply just as well to a coupled atmosphere–ocean model as to the real planet. Thus, it would imply that in the climatology of coupled GCMs, LWCRF and SWCRF might be individually biased, but that these biases should compensate. In particular, one might expect LWCRF and SWCRF to compensate better in the coupled climate than in a specified-SST GCM simulation, which does not support the Hartmann et al. mechanism. This would be an interesting test to perform on a suite of coupled models.

A second test would be to look at compensation of LWCRF and SWCRF in cloud-resolving models (CRMs) run to radiative-convective equilibrium in different climates. Tompkins and Craig (1999) performed such simulations in doubly-periodic domains above SSTs of 298, 300 and 302 K. They found approximate compensation between LWCRF and SWCRF in all simulations. Since this setup did not include any horizontal variations, it excludes the Hartmann et al. mechanism, yet reproduces the SWCRF-LWCRF compensation. Bretherton (2007) discussed a CRM analogue to the idealized Walker circulation model discussed in the previous section. In that simulation, LWCRF was approximately 70% as large as SWCRF throughout the simulated region of deep convection (P. Blossey, pers. comm.), so there was no compensation of the two cloud forcings even in a domain-averaged sense. The difference between the ratio of LWCRF/SWCRF in this simulation and those of Tompkins and Craig suggests that this ratio is strongly affected by CRM microphysical parameterizations. Both of these CRM studies favor a Kiehl-type argument, but further CRM study of the control of LWCRF/SWCRF in tropical oceanic deep convection is warranted.

Boundary Layer Cloud and Lower Tropospheric Stability

Lower tropospheric stability is a good predictor of boundary layer cloud impacts on atmospheric and surface radiation balance, as encapsulated in Equation 10.2. Can this relation be quantitatively extended to other climates? If so, this would provide an important step toward understanding low cloud feedbacks on climate sensitivity.

Physically, one can argue that this relation reflects how the typical thermodynamic profile of the lower troposphere changes between stratocumulus and

shallow cumulus cloud regimes. Marine stratocumulus clouds tend to have a low, strong capping inversion. The strong inversion inhibits entrainment of dry air from above, and the low inversion top allows a well-mixed turbulent cloud-topped layer to persist. The strong inversion and thick layer of stable stratification between this inversion and 700 hPa both contribute to large LTS. If the inversion is weaker, entrainment tends to deepen the boundary layer, which then decouples into a cumuliform structure with less cloud just below the capping inversion. The weaker, higher inversion leads to smaller S . This argument would apply to other climates, but not necessarily with the same constants as in Equation 10.2.

In a warmer climate, LTS tends to increase across the tropics. The free tropospheric stratification, which is determined mainly by deep convection over the warmest parts of the tropics, roughly follows a moist adiabat. In a warmer climate, the moist adiabatic $d\theta/dz$ increases, contributing to an increase in LTS. Does this then increase low cloud amount and act as a negative climate feedback? GCM simulations by Medeiros et al. (2008) show that if tropical SSTs are uniformly warmed by 2 K, then low cloud cover is largely unaltered despite increased LTS across the entire tropics. One could represent this in Equation 10.2 by a shift toward higher LTS_q in the warmer climate.

Wood and Bretherton (2006) proposed a variant on LTS, called Estimated Inversion Strength (EIS), which removes the effect of free-tropospheric stratification changes that track a moist adiabat. EIS correlates very well with LTS across the low-latitude oceans, but is a better predictor than LTS of stratus cloud fraction over the midlatitude oceans. In these regions, the free-tropospheric stratification tracks a cooler adiabat than in the tropics. This suggests that EIS might also be a “climate-invariant” low cloud predictor, which might be applicable to other climates with perturbed moist adiabats. This hypothesis could be tested using carefully designed sensitivity studies with large-eddy simulations of boundary layer clouds.

Modeling Clouds in Large-scale Circulations

Cloud feedbacks on large-scale circulations are a challenge for GCMs. They involve complex interactions between resolved-scale fields and a suite of parameterized moist processes, including microphysics, cloud fraction, cumulus convection, boundary layer turbulence, surface fluxes, and radiation. In low latitudes, almost all clouds are intimately associated with some form of convection and turbulence. Even in extratropical cyclones, the ice and liquid water paths in the main region of large-scale ascent will be sensitive to microphysical parameterization uncertainties; there will certainly be turbulence-driven boundary layer clouds (convective behind the cold front, possibly shear-driven in the warm sector) and possibly also embedded deep convection. Designing a single parameterization to respond correctly to the full range of large-scale conditions

encountered around the globe is challenging; to design and improve a system of tightly coupled parameterizations that work together as intended is even more so. Furthermore, many clouds are thin, and hence poorly resolved by the vertical grid of a typical GCM. The parameterization of cloud–aerosol interactions adds another layer to the challenge. Hence, results derived from GCMs about cloud–aerosol interaction and cloud feedbacks should be critically analyzed and traced to plausible and testable physical mechanisms before they are taken too seriously.

Global models that resolve the cloud processes at much higher spatial resolution may help with these challenges. In a GCM, in which grid spacing typically exceeds 100 km, there is often enormous horizontal cloud heterogeneity within grid cells. The moist physical parameterizations must be aggregated to the grid-cell scale at which they interact using assumptions about this heterogeneity. In practice, the heterogeneity is rarely treated in a fully consistent manner across all parameterizations, leading to such non-sequiturs as rain with no cloud.

It is much more appealing if the cloud physical parameterizations and dynamics can interact at the scale of individual eddies, within which horizontal heterogeneity is not as severe. This explains the success of large-eddy simulation (using grid resolutions of 100 m or less to simulated boundary layer cloud systems) and cloud-resolving modeling (using resolution of 1–5 km to simulate deep convective cloud systems). Global climate CRMs are in their infancy, but they show promise and are already being applied to study cloud-radiative responses on global scales (see Collins and Satoh, this volume). Global and regional numerical weather prediction models are being run without deep cumulus parameterizations at similar or better resolutions. Super-parameterization (Grabowski and Petch, this volume) is a shortcut to a global CRM: a small CRM is placed at each grid column of a GCM, and the CRMs interact through their averaged effects on the GCM grid. As with a global CRM, the cloud processes in a super-parameterized GCM interact on the large-eddy scale. Although super-parameterization involves roughly 100-fold more computations than a regular GCM, it is much cheaper than a full global CRM of the same resolution. A potential advantage of super-parameterization over a global CRM is that the CRM resolution in a super-parameterization can be made much finer or even customized to the geographic location or weather regime, making global cloud-resolving simulations of boundary layer clouds and their cloud and aerosol feedbacks possible. However, current super-parameterizations use 4 km horizontal resolution, which is inadequate for this purpose. None of these global high-resolution simulation methods resolve all cloud processes, and all involve uncertain microphysical and other parameterizations (see Grabowski and Petch, this volume). Hence there is no guarantee that they could represent clouds or their interactions with large-scale circulations much better than a conventional GCM; there are still significant biases in their simulated climate and cloud climatology (e.g., Khairoutdinov and Randall 2005). Thus we return

to observational tests of how well models of all types simulate different cloud regimes and their relation to large-scale dynamics.

Biases in the PDFs of the vertical distribution and thickness of clouds are of particular relevance to modeling cloud–aerosol interaction and cloud feedbacks, because simulated clouds with biased vertical structure can be expected to show a distorted response to changes in aerosol, temperature, or vertical motion. Zhang et al. (2005) and Wyant et al. (2006a, b) documented such biases by applying an “ISCCP simulator” to model output; this partitions clouds by their cloud-top pressure and cloud optical depth to mimic a similar ISCCP satellite-derived dataset.

Zhang et al. (2005) segregated results into latitude belts to examine different cloud regimes. Wyant et al. (2006a) used “Bony-binning,” in which monthly-mean ω_{500} is used to sort low-latitude clouds into dynamic regimes. Mean ascent ($\omega_{500} < 0$) favors deep convection, and mean subsidence ($\omega_{500} > 0$) favors boundary layer cloud. Figure 10.7 (from Wyant et al. 2006b) applies this approach to compare ISCCP-like cloud statistics from two conventional GCMs and a super-parameterized GCM with satellite observations. All three models simulate too little optically thin cloud, except at the tropopause, and too much optically thick cloud at all levels. For tropical deep convective regimes, con-

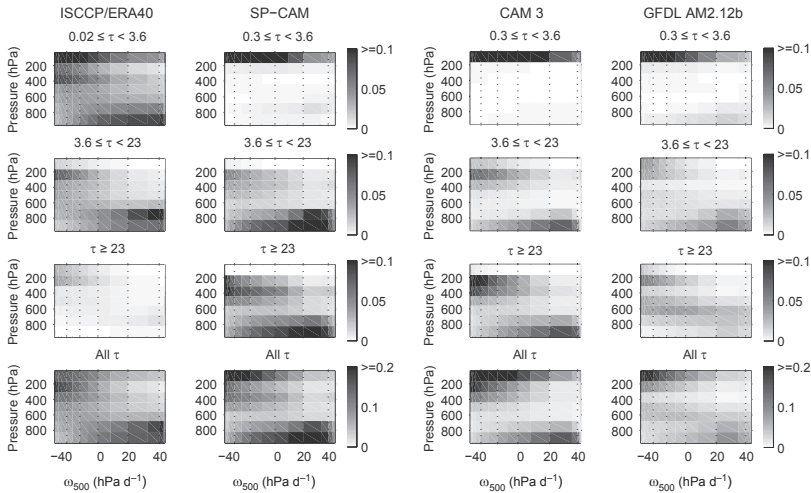


Figure 10.7 Probability distribution of cloud-top pressure conditional on monthly mean ω_{500} based on all grid-column months in 30°S – 30°N . Rows show partitioning into thin, medium, and thick optical depth categories. Bottom row includes all cloud optical depths, τ . Left column: ISCCP observations. Other columns show model-derived ISCCP simulator results from super-parameterized CAM-SP and the CAM3 and AM2 GCMs. ω_{500} scale stretched to show frequency of occurrence. Adapted from Fig. S1 in Wyant et al. (2006b).

ventional GCMs also underestimate mid-topped cloud in ascent regimes; the super-parameterized GCM reduces this bias.

Another well-known bias of most GCMs is that the diurnal cycle of cumulus convection is advanced by several hours compared to observations (e.g., Yang and Slingo 2001). Because cumulus convection releases latent heat, this results in continental-scale feedbacks with vertical motion over the tropics. Again, super-parameterization reduces this bias (Khairoutdinov et al. 2005).

We have emphasized the limits of our ability to model accurately the interaction of clouds and dynamics in the current climate. These limits relate closely to our lack of fundamental understanding of the empirical controls on tropical deep and low cloud forcing. New tools, such as cloud-resolving global modeling, and new observations, such as the NASA A-Train suite as well as new efforts to mine the historical data record, may lead to progress if cleverly applied, but no pat answer is in sight. Therefore, we must tread carefully and test comprehensively as we add processes to global climate models, such as aerosols and chemistry, which interact closely with clouds.

Acknowledgments

The authors acknowledge support from NASA grant NNG05GA19G and NSF grant ATM-0336703 for research presented herein. We would like to thank Matt Wyant and Larissa Back for redrafting figures for use in this paper, and Jost Heintzenberg, Anthony Illingworth, Jon Petch, Yukari Takayabu, Rob Wood, and an anonymous reviewer for helpful comments.

References

- Back, L. E., and C. S. Bretherton. 2006. Geographic variability in the export of moist static energy and vertical motion profiles in the tropical Pacific. *Geophys. Res. Lett.* **33**:L17810.
- Barsugli, J. J., S. I. Shin, and P. D. Sardeshmukh. 2006. Sensitivity of global warming to the pattern of tropical ocean warming. *Climate Dyn.* **27**:483–492.
- Bony, S., and J.-L. Dufresne. 2005. Marine boundary layer clouds at the heart of cloud feedback uncertainties in climate models. *Geophys. Res. Lett.* **32**:L20806.
- Bretherton, C. S. 2007. Challenges in numerical modeling of tropical circulations. In: *The Global Circulation of the Atmosphere*, ed. T. Schneider and A. H. Sobel, pp. 302–330. Princeton: Princeton Univ. Press.
- Gregory, J., and M. J. Webb. 2008. Tropospheric adjustment induces a cloud component in CO₂ forcing. *J. Climate* **21**:58–71.
- Hartmann, D. L., and K. Larson. 2002. An important constraint on tropical cloud–climate feedback. *Geophys. Res. Lett.* **29**(20):1951.
- Hartmann, D. L., L. Moy, and Q. Fu. 2001. Tropical convection and the energy balance at the top of the atmosphere. *J. Climate* **14**:4495–4511.
- Held, I. M., and B. J. Soden. 2006. Robust responses of the hydrological cycle to global warming. *J. Climate* **19**:5686–5699.

- Khairoutdinov, M. F., C. DeMott, and D. A. Randall. 2005. Simulation of the atmospheric general circulation using a cloud-resolving model as a super-parameterization of physical processes. *J. Atmos. Sci.* **62**:2136–2154.
- Kiehl, J. T. 1994. On the observed near cancellation between longwave and shortwave cloud forcing in tropical regions. *J. Climate* **7**:559–565.
- Klein, S. A., and D. L. Hartmann. 1993. The seasonal cycle of low stratiform clouds. *J. Climate* **6**:1587–1606.
- Kubar, T. L., D. L. Hartmann, and R. Wood. 2007. Radiative and convective driving of tropical high clouds. *J. Climate* **20**:5510–5526.
- Medeiros, B. P., B. Stevens, I. M. Held et al. 2008. Aquaplanets, climate sensitivity and low clouds. *J. Climate*, in press.
- Neelin, J. D., and N. Zeng. 2000. A quasi-equilibrium tropical circulation model formulation. *J. Atmos. Sci.* **57**:1741–1766.
- Peters, M. E., and C. S. Bretherton. 2005. A simplified model of the Walker circulation with an interactive ocean mixed layer and cloud-radiative feedbacks. *J. Climate* **18**:4216–4234.
- Ramanathan, V., and W. Collins. 1991. Thermodynamic regulation of ocean warming by cirrus clouds deduced from observations of the 1987 El Niño. *Nature* **351**:27–32.
- Rossow, W. B., and R. A. Schiffer. 1999. Advances in understanding clouds from ISCCP. *Bull. Amer. Meteor. Soc.* **80**:2261–2287.
- Seager, R., M. F. Ting, I. Held et al. 2007. Model projections of an imminent transition to a more arid climate in southwestern North America. *Science* **316**:1181–1184.
- Tompkins, A. M., and G. C. Craig. 1999. Sensitivity of tropical convection to sea surface temperature in the absence of large-scale flow. *J. Climate* **12**:462–476.
- Vecchi, G. A., B. J. Soden, A. T. Wittenberg et al. 2006. Weakening of tropical Pacific atmospheric circulation due to anthropogenic forcing. *Nature* **441**:73–76.
- Waliser, D. E., and N. E. Graham. 1993. Convective cloud systems and warm-pool sea surface temperatures: Coupled interactions and self-regulation. *J. Geophys. Res.* **98**:12881–12893.
- Wood, R., and C. S. Bretherton. 2006. On the relationship between stratiform low cloud cover and lower tropospheric stability. *J. Climate* **19**:6425–6432.
- Wyant, M. C., C. S. Bretherton, J. T. Bacmeister et al. 2006a. A comparison of tropical cloud properties and responses in GCMs using mid-tropospheric vertical velocity. *Climate Dyn.* **27**:261–279.
- Wyant, M. C., M. Khairoutdinov, and C. S. Bretherton. 2006b. Climate sensitivity and cloud response of a GCM with a superparameterization. *Geophys. Res. Lett.* **33**:L06714.
- Xie, P., and P. A. Arkin. 1997. Global precipitation: A 17-year monthly analysis based on gauge observations, satellite estimates, and numerical model outputs. *Bull. Amer. Meteor. Soc.* **78**:2539–2558.
- Yang, G.-Y., and J. Slingo. 2001. The diurnal cycle in the tropics. *Mon. Wea. Rev.* **129**:784–801.
- Yin, J. H. 2005. A consistent poleward shift of the storm tracks in simulations of 21st century climate. *Geophys. Res. Lett.* **32**:L18701.
- Zhang, M. H., W. Y. Lin, and S. A. Klein et al. 2005. Comparing clouds and their seasonal variations in 10 atmospheric general circulation models with satellite measurements. *J. Geophys. Res.* **110**:D15S02.
- Zhang, Y. C., W. B. Rossow, A. A. Lacis, V. Oinas, and M.I. Mishchenko. 2004. Calculation of radiative fluxes from the surface to top of atmosphere based on

- ISCCP and other global datasets: Refinements of the radiative transfer model and the input data. *J. Geophys. Res.* **109**:D19105.
- Zhu, P., J. J. Hack, J. T. Kiehl, and C. S. Bretherton. 2007. Climate sensitivity of tropical and subtropical marine low cloud amount to ENSO and global warming due to doubled CO₂. *J. Geophys. Res.* **112**:D17108.